Lubrication and Wear Protection of Micro-Structured Hydrogels using Bioinspired Fluids

Jimmy Faivre[1,2], Alexandra Montembault[1], Guillaume Sudre[1], Buddha Ratna Shrestha[2], Guojun Xie[3], Krzysztof Matyjaszewski[3], Stéphane Benayoun[4], Xavier Banquy[2], Thierry Delair[1], Laurent David[1*]*

[1]*Ingénierie des Matériaux Polymères, IMP- CNRS UMR 5223, Université de Lyon, Université Claude Bernard Lyon 1, 15 Boulevard Latarjet, 69622 Villeurbanne Cedex, France*

[2]*Canadian Research Chair in Bioinspired materials, Faculty of Pharmacy, Université de Montréal, Montréal, Qc, Canada*

[3]*Center for Macromolecular Engineering, Department of Chemistry, Carnegie Mellon University, Pittsburgh, PA, USA*

[4]*Laboratoire de Tribologie et Dynamique des Systèmes, CNRS UMR 5513, Ecole Centrale de Lyon, 36 Avenue Guy de Collongue, 69134 Ecully Cedex, France*

Abstract

We report the fabrication and the use of a bioinspired synovial fluid acting as a lubricant fluid and anti-wear agent at soft and porous chitosan hydrogel tribopairs. This synthetic synovial fluid is composed of sodium hyaluronate (HA) and a bottle-brush polymer (BB) having a polycationic attachment group and polyzwitterionic pendant chains. 2.5 $\%_{w/w}$ chitosan hydrogel plugs are organized in a bilayered structure exposing a thin and dense superficial zone (SZ), covering a porous deep zone (DZ) and exhibiting microchannels perpendicularly aligned to the SZ. Using a low-load tribometer, the addition of HA lubricating solution at the hydrogel-hydrogel rubbing contact drastically decreased the coefficient of friction (CoF) from $\mu = 0.20 \pm 0.01$ to $\mu = 0.04 \pm 0.01$ on the DZ configuration and from $\mu = 0.31 \pm 0.01$ to $\mu = 0.08 \pm 0.01$ on the SZ surface when increasing HA concentration from 0 to 1000 µg/mL and its molecular mass from 10 to 1500 kDa, similar to what was found when using BB polymer alone. When combining the BB polymer and the 1500 kDa HA, the CoF remained stable at $\mu = 0.04 \pm 0.01$ for both studied contact configurations, highlighting the synergistic interaction of the two macromolecules. Hydrogel wear was characterized by assessing the final gel surface roughness by the means of an interferometer. Increasing HA concentration and molecular weight plus the addition of BB polymer lead to a dramatic surface wear protection with a final gel surface roughness of the hydrogels similar to the untested gels. In brief, BB polymer in combination with high molecular weight HA is a potential lubricating fluid as well as a wear resistant agent for soft materials lubrication and wear protection.

Keywords: hydrogel lubrication, wear resistance, chitosan, bottlebrush polymer, hyaluronic acid

1.Introduction

Hydrogels are of growing interest for tissue engineering as scaffolds since they can structurally and mechanically mimic the tissues and embed growth factors as well as chondrocytes to support joint regeneration[1-3]. However, few *in vivo* studies have characterized the potential lubrication properties and wear protection abilities of hydrogels despite its paramount importance for tissue engineering sustainability. For instance, in healthy diarthrodial joints, the cartilage and the synovial fluid act in synergy to provide low coefficient of friction (CoF) and excellent wear protection[4-8]. This synergy leads to efficient multiple modes of lubrication, depending on the spatio-temporal configuration of the joint during the motion process[9]. The excellent wear resistance is due to the fluid pressurization within the cartilage[10] and the presence of aggrecan (Agg)-hyaluronic acid complexes which increase the osmotic pressure within the collagen matrix which helps supporting the load[11-12]. Moreover, the formation of a thin macromolecular layer on the cartilage surface under load avoids the cartilage surfaces from rubbing on each other. To ameliorate lubrication and alleviate mechanical erosion of soft synthetic materials used as *in vivo* tissue substitutes, different bio-inspired strategies have been described in the literature. Indeed, the friction forces of hydrogels surfaces can be modulated *via* their surface porosity[13], topography[14-15] or the presence of highly hydrated moieties on polymer groups[16-17]. For instance, Lin *et al*. showed a CoF of $\mu = 0.15$ by using bilayered hydrogels made of a mixture of acrylamide, acrylic acid and diacrylamide exposing a highly porous superficial layer compared to a denser structure with a CoF of $\mu = 0.35$ [13]. The insertion of hydrophilic [2-(methacryloyloxy)ethyl] trimethylammonium chloride as part of the gel matrix drastically reduced the CoF to 0.05 thanks to the higher water trapping capability of the charged polyelectrolyte. The design of vertical pores or fibers at hydrogel surfaces is another technique to allow better lubrication

due to water exudation upon compression and thus the formation of a lubricating hydrodynamic film[15, 18], a technique which can be combined with highly hydrophilic monomers[19]. To drastically decrease CoF, another method is to directly graft polyelectrolyte brushes at the gel surface. For example, poly(sodium 4-styrene sulfonate) grafted to poly(hydroxyethyl methacrylate) (p(HEMA)) lowered by almost an order of magnitude the CoF of p(HEMA) hydrogels[20]. The friction can also be decreased upon addition of a lubricating fluid either composed of surfactants[21], lipids, or naturally-occurring or bioinspired proteoglycans[22], which are known to be responsible for the lubrication and wear protection of eyes, joints or mucous membranes. Nevertheless, the tools used for the tribological measurement such as tribometers or rheometers, the geometry of the probe (pin or ball on disc), the contact area or the nature and roughness of opposing geometry (glass, metal or hydrogel), highly affects the results and hence should be meticulously described in order to be comparable to other studies.

On the other hand, the interest on wear protection of soft materials is growing since it is essential to ensure the integrity of the hydrogels scaffolds to fully sustain the physiological conditions (pressure, shear, inflammation). The main route to limit wear initiation to hydrogels is to strengthen the scaffold *via* crosslinking[23] or interpenetrated networks[24-25]. An interesting alternative is called the "sacrificial bond principle"[26] which is based on the insertion of weak bonds inside the initial gel matrix. When a crack propagates in the gel, the weaker bonds break first and dissipate a large amount of energy[27]. Finally, the total energy needed to damage the hydrogels is drastically increased by several orders of magnitude compared to their counterparts without any sacrificial bonds.

In the present study, we emphasize on the design of lubricating fluids which are able to lubricate *and* reduce wear at soft multilayered chitosan hydrogels. These lubricating fluids

were previously proven to reduce both friction and wear of stiff and non porous mica surfaces with CoF of $\mu \sim 0.02$ up to pressures of several megaspascals[28], matching physiological conditions. Contrary to mica surfaces, poroelastic chitosan hydrogels more closely mimic soft tissues, but ~~and~~ suffer from frictional abrasion at low stresses impeding their uses *in vivo*[18]. By using a low-load tribometer and light interferometry, we show that the addition of high molecular weight hyaluronic acid (HA) and bottlebrush (BB), polymer at the interface between the two sliding chitosan gel tribopairs significantly lowered both the CoF and wear for both studied surface topographies. BB polymers represent novel polymeric architecture with very densely grafted side chains[29] which are typically prepared by atom transfer radical polymerization[30]. This unique architecture resembles the proteoglycan lubricin structure which is involved in the lubrication of the synovial joints. Since the synovial fluid also contains hyaluronic acid and phospholipids (DPPC)[31] the combination of HA with a synthetic BB polymer composed of pendant phospholipids moieties[32] mimics the macromolecular structure and composition of synovial fluid. This leads to the concept of bioinspired synovial fluids. This work demonstrates the potentiality of this lubricant and anti-wear fluid to help hydrate physiological surfaces such as in the case of dry eye syndrome or tissue substitutes such as contact lenses or cartilage substitutes to keep and extend their tribological properties *in vivo*.

2. Experimental Section

2.1. Materials

Chitosan (M_w = 6.04.10^5, M_w/M_n 1.6, DA 4.5%, from squid pen chitin) was purchased from Mahtani Chitosan Pvt. Ltd (batch type 114). Sodium hyaluronates of different molecular weights were obtained from Lifecore Biomedical (Minneapolis, USA). Acetic acid, ammoniac hydroxide, and HEPES were supplied by Sigma-Aldrich. NaOH pellets, NaCl, and absolute anhydrous ethanol were obtained from Carlo Erba Reagents. Methyl methacrylate (MMA, 99%, Sigma-Aldrich), 2-(trimethylsilyloxy)ethyl methacrylate (HEMA-TMS, 96%, Sigma-Aldrich) and 2-(dimethylamino)ethyl methacrylate (DMAEMA, 98%, Sigma-Aldrich) were passed through a column filled with basic alumina prior to use. 2-Methacryloyloxyethyl phosphorylcholine (MPC, 97%, Aldrich) was recrystallized from acetonitrile and dried under vacuum overnight at room temperature before polymerization. Copper(I) bromide (Cu^IBr, 99.999%, Sigma-Aldrich), copper(II) bromide ($Cu^{II}Br_2$, 99.999%, Sigma-Aldrich), copper(I) chloride (Cu^ICl, ≥99.999% trace metals basis, Alfa Aesar), copper(II) chloride ($Cu^{II}Cl_2$, ≥99.999% trace metals basis, Sigma-Aldrich), 2,2′-bipyridyl (bpy, 99%, Sigma-Aldrich), 4,4′-Dinonyl-2,2′-dipyridyl (dNbpy, 97%, Sigma-Aldrich), potassium fluoride (KF, 99%, Sigma-Aldrich), tetrabutylamonium fluoride (TBAF, 1M solution in THF, Sigma-Aldrich), bromoisobutyryl bromide (BBiB, 98%, Sigma-Aldrich), α-bromoisobutyryl bromide (98%, Sigma-Aldrich), bromoethane (98%, Alfa Aesar), tris(2-pyridylmethyl)amine (TPMA) (98%, Sigma-Aldrich), and tributyltin hydride (97%, Sigma-Aldrich) were used without any additional purification. Solvents were used as received.

2.2. Chitosan hydrogels fabrication

Prior to gel fabrication, chitosan was purified by filtration on Millipore membranes of decreasing porosity (membrane porosities of successively 3, 0.8, and 0.45μm). 2.5 $\%_{w/w}$

multilayered chitosan physical hydrogels were fabricated according to previously published procedure[18]. In short, 2.5%$_{w/w}$ solution was prepared by dissolving chitosan purified powder with a stoichiometric amount of acetic acid in water. The chitosan solution was then centrifuged at 5000 rpm for 10 min to remove air bubbles. The solution was then extruded and deposited on a plastic foil and pressed with a metal plate with 1.5 mm wedges to maintain the same thickness in all gels (i.e. 1.5 mm). The viscous chitosan film was then placed in a NaOH coagulation bath at 1 mol/L until the completion of the gelation process. The resulting gel disks were cut with a punch to final diameters of 11 and 21mm. The gel disks were washed in pure water to reach neutral pH. The nano and micro structure of physical 2.5%$_{w/w}$ chitosan hydrogel were assessed by confocal microscopy (CLSM) and Scanning Electron Microscopy (SEM).

2.3. BB Polymer synthesis

In the following section, we describe the synthesis of the BB polymer of final composition **[(PBiBEM$_{552}$-*g*-PMPC$_{45}$)-*stat*-MMA$_{338}$]-*b*-(PqDMAEMA$_{93}$-*stat*-PMMA$_{153}$)** whose structure is inspired by our previously published references [32-34].

Synthesis of P(HEMA-TMS)-*stat*-PMMA (A block (Fig. 1A)): A dried round bottom flask was charged with BBiB (3.4 µL, 0.023 mmol), dNbpy (112.8 mg, 0.276 mmol), HEMA-TMS (10.0 mL, 45.9 mmol), MMA (4.9 mL, 45.9 mmol) and anisole (3.0 mL). The solution was bubbled with argon for 30'. Cu^{I}Br (0.0158 g, 0.110 mmol), and Cu^{II}Br$_2$ (0.0061 g, 0.028 mmol) were charged in a dried 50 mL round bottom flask and 3 argon-vacuum cycles were performed to remove oxygen. The flask was sealed, and then immersed in an oil bath at 40 °C. After bubbling, the monomer solution was injected into the catalyst solution. Reaction was stopped after 14 h via exposure to air, reaching the degree of polymerization of the product 500. The monomers consumption was calculated from ^{1}H NMR spectra by the

integration of MMA and HEMA-TMS vinyl groups signal (C*H*H=C-CH_3, 6.11 ppm or 5.56 ppm) against the internal standard (anisole, *o*,*p*-Ar-H, 6.91 ppm). The product **A** was purified by three precipitations from methanol, dried under vacuum overnight at room temperature, and analyzed by GPC and ^{1}H NMR spectroscopy. The ratio of PMMA (*s*, broad, CO-O-CH_3, 3.54-3.68 ppm) to P(HEMA-TMS) (*s*, broad, OCO-CH_2, 3.90-4.17 ppm) signals gave the polymer composition.

Synthesis of (PDMAEMA-*stat*-PMMA)-*b*-[P(HEMA-TMS-*stat*-PMMA] (BA diblock (Fig. 1A)): A dried round bottom flask was charged with **A block** (1.0 g, 0.0094 mmol), dNbpy (70 mg, 0.17 mmol), DMAEMA (1.2 mL, 7.0mmol), MMA (0.75 mL, 7.0 mmol) and anisole (4.0 mL). The solution was bubbled with argon for 30'. $Cu^{I}Cl$ (0.0074 g, 0.0752 mmol), and $Cu^{II}Cl_2$ (0.0010 g, 7.46 μmol) were charged in a dried 25 mL round bottom flask and 3 argon-vacuum cycles were performed to remove oxygen. The flask was sealed, and then immersed in an oil bath at 60 °C. After bubbling, the monomer solution was injected into the catalyst solution. Reaction was stopped after 48 h via exposure to air. The product was diluted in dichloromethane, passed through a neutral alumina column, concentrated under vacuum and precipitated twice from hexanes and water. The solvent was removed under vacuum and the product was dried overnight under vacuum at room temperature. The structure of the polymer was determined by ^{1}H NMR from the ratio of selected polymer signals: PMMA (*s*, broad, CO-O-CH_3, 3.54-3.68 ppm),P(HEMA-TMS) (*s*, broad, O-Si(CH_3)$_3$, 0.11-0.21 ppm) and PDMAEMA (*m*, CH_2-NMe_2, 2.55-2.65 ppm).

Synthesis of [PBiBEM-*stat*-PMMA]-*b*-(PqDMAEMA-*stat*-PMMA) (BA-Macroinitiator (BA-MI)): BA diblock (0.1840 g), potassium fluoride (0.030 g, 0.52 mmol) and 2,6-di-*tert*-butylphenol (0.0090 g, 0.0439 mmol) were placed in a 20 ml round bottom flask. The flask was sealed, flushed with argon, and finally anhydrous THF (7 mL) was added. The mixture

was cooled in an ice bath to 0 °C, tetrabutylammonium fluoride solution in THF (1M, 0.44 mL, 0.44mmol) was injected into the flask, followed by a drop-wise addition of 2-bromoisobutyryl bromide (0.121 g, 65 μL, 0.526mmol). After the addition, the reaction mixture was allowed to reach room temperature and stirring was continued for 24 h. The solution was passed through a short column filled with basic alumina, precipitated into hexanes and then methanol:water (70:30, v/v%) three times. The filtrate was dried under vacuum overnight at room temperature.

Synthesis of [(PBiBEM-*g*-PMPC)-*stat*-MMA]-*b*-(PDMAEMA-*stat*-PMMA) (BAC polymer (Fig. 1A)): A dry 10 mL round bottom flask was charged with polymer **BA-MI** (2mg), 2-methacryloyloxyethyl phosphorylcholine (MPC)(0.2540 g, 0.860mmol), 2,2'-bipyridyl (bpy) (22 mg, 14.23 μmol), $Cu^{I}Cl$ (6 mg, 60 μmol), and copper (II) chloride ($Cu^{II}Cl_2$) (1 mg, 7.40 μmol). A dry 10 mL round bottom flask was charged with methanol (3.0 mL) and anisole (500 μL). The solution was bubbled with argon for 15 min. The flask was sealed, and then immersed in an oil bath at 50 °C. After bubbling, the solvent solution was injected into the catalyst/monomer solution. Time of reaction was determined thanks to MPC conversion measurement by ^{1}H NMR to reach a DP of 45. Reaction was then stopped via exposure to air achieving PMPC diblock brush. The resulting brush was purified by ultrafiltration against MeOH under pressure using regenerated cellulose membrane (Millipore) with a pore size molar mass cut-off of 30,000 Da. Molecular weights were not determined as polymer was neither soluble in THF nor in DMF.

Synthesis of [(PBiBEM-*g*-PMPC)-*stat*-MMA]-*b*-(PqDMAEMA-*stat*-PMMA) (BB polymer)): BAC was placed in 20 mL vial and dissolved in methanol (10 mL). The solution was cooled in an ice bath to 0 °C, followed by a slow addition of bromoethane (0.5mL, 6.7 mmol). The reaction was stirred at room temperature for the next 48 h. The solvent and the

unreacted bromoethane were evaporated under gentle pressure and solvent was exchanged for water by ultrafiltration. The polymer was freeze-dried and stored at -20°C in a dark container. The quantitative quaternization of -NMe_2 groups of **BB polymer** was determined by ^1H NMR.

2.4. Equipment and Analysis

Proton nuclear magnetic resonance (^1H NMR) spectroscopy was performed using Variant 400 MHz spectrometer. In all cases, deuterated chloroform ($CDCl_3$) was used as a solvent, except for PMPC ABA which was analyzed using deuterated water (D_2O). ^1H chemical shifts are reported in ppm downfield from tetramethylsilane (TMS) in deuterated chloroform and from 3-(trimethylsilyl) propane sulfonate sodium salts in deuterated water. Apparent molecular weights and molecular weight distributions measurements of polymers were measured by gel permeation chromatography (GPC, Waters 1525 system 35°) using Phenogel columns (guard, 10^5, 10^4, and 10^3 Å), with THF or DMF as eluent at 35 °C at a constant flow rate of 1.00 mL/min, and differential refractive index (RI) detector (Waters, 2414). The apparent number-average molecular weights (M_n) and molecular weight distribution (M_w/M_n) were determined with a calibration based on linear poly(styrene) (PS) standards (Polyscience).

AFM measurements were collected using a multimode Atomic Force Microscopy (AFM) with a NanoScope V controller (Bruker) in PeakForce QNM mode. Silicon tips (on nitride cantilever) with resonance frequency of 50-90 kHz and spring constant of ~0.4 N/m were used. The samples were dissolved in water and deposited on freshly cleaved mica.

2.5. Formulation of synthetic synovial fluids

10.0 mg of different molecular mass HA (10, 60, 500, and 1500 kDa) were dissolved with magnetic stirring in 10 mL 0.1M HEPES buffer pH 7.4 in a glass vial. The solution was then

immediately poured in the tribometer bath immersing chitosan hydrogels during wear test. For tests with B-B polymer, 100 or 400 µg/mL solutions of B-B polymer were prepared in the same buffer with or without HA. Solutions were homogenized with a vortex for 1 min. Surfaces were then let to equilibrate for 1 h prior to the measurements.

2.6. Tribology tests on hydrogel tribopairs

A low load tribometer was used to assess frictional properties of chitosan gels in presence of artificial synovial fluids. The 11 mm gel disk was glued on the top mobile part on an aluminum pin and was able to rotate and be adjusted *via* a ball joint to obtain a flat contact between both gels. The 21 mm gel disk was glued on a metallic immobile metal surface. Typically, the two gel disks were pressed against each other reaching the set load and the mobile part was driven to oscillate at a frequency of 1 Hz with an amplitude of 5 mm from 500 to 1000 cycles. Normal and tangential forces were recorded and analyzed using a home-made labview software. Gels were glued on the mobile top part and immobile bottom part with Loctite Super Glue 3 power flex gel (from Loctite, waterproof and suited for porous materials). Two different configurations of the gel disks were characterized: 1) SZ on SZ flat contact and 2) DZ on DZ flat contact. During the experiments, the disks were fully immersed in the synthesized synovial fluid. Friction force (F_t) measurements were firstly performed as a function of the sliding velocity (v) with a constant load (F_n = 0.3 N) (0.3 N corresponding to a stress of 3 kPa which represents 10 % of elastic shear modulus of the gel G' determined at a frequency of 1Hz) and at an amplitude of 5 mm. This normal load was chosen to avoid the destruction of the gel under shearing at the DZ/DZ configuration which was systematically noticed at a pressure close to the shear modulus[18]. The number of cycles was increased to adapt the length of the experiments throughout the friction experiments as a function of sliding velocity since we covered three decades of velocities from 0.1 to 100 mm/s. In a

second step, the effect of normal force was assessed at a sliding frequency of 1 Hz and an amplitude of 5 mm for 250 cycles. The range of applied normal forces was between 0.05 N and 5 N. Finally, wear of the gel disks was evaluated after shearing the surfaces for 10^4 cycles (at F_n = 3 N, P = 30 kPa, and v = 5 mm/s). Wear was visualized using a digital microscope (VHX-1000, Keyence) for optical micrographs and an interferometric microscope (Contour GT-K 3D Bruker). Surface roughness was characterized by the arithmetical mean height (S_a) of the surface and was quantified using vision 64 software (Bruker). The surface analyzed for the roughness measurements represented 20% of the total contact area. Prior to wear visualization, samples were dried by blowing compressed air to improve imaging contrast.

2.7. Correlation with physiological conditions

All experimental setups and parameters were adjusted to match physiological conditions as often as possible. pH was adjusted to 7.4 as in human fluids. The sliding frequency was in the range of 0.01 to 100 mm/s, similar to normal knee, eyelid or airways cilium motion speed[35-39], with a displacement of 5 mm. The gel on gel plate geometry was placed in a bath filled with synthetic fluids in order to match natural synovial joints (i.e. cartilage on cartilage contact within synovial fluid) or eyes/eyelids/contact lenses function. Finally, the physical chitosan gel layered-structure composed of a thin superficial zone supported by a network of channels of few micrometers in diameter and perpendicularly orientated to the superficial zone was previously mechanically studied[40] and was proven to be an interesting tribological surface model to mimic natural tissues.

3. Results & Discussions

3.1. Experiment Design

The bioinspired synovial fluid was formulated using a BB polymer and HA in a buffered solution. The BB polymer is composed of three different blocks: a A block which is the polymer backbone bearing lateral chains, a polycationic B block - linked to the backbone - which provides attachment to negatively charged surfaces and the lateral C blocks - constituted of phosphoryl choline moieties acting as hydrophilic pendant chains (Fig. 1A). The different constituents of the synthetic synovial fluids were introduced at concentrations close to natural joints for proteoglycans and HA. BB polymer concentration was 400 µg/mL whereas HA was used at concentrations ranging from 10 to 1000 µg/mL[41-43]. HA molecular mass was selected from 1.5 MDa, representing near physiological HA molecular mass, to 10 kDa which is close to degraded HA molecular weight[44]. The substrates used as tribopairs were 2.5 $\%_{w/w}$ chitosan hydrogels whose structure and mechanical behavior were previously characterized[18, 45-47]. The hydrogels were analyzed using confocal microscopy and SEM imaging (Fig. 1B). They exhibited a bilayer structure with a first ~ 100 µm dense layer membrane called superficial zone (SZ). The SZ covered a deep zone (DZ) forming the majority of the gel disks composed of microchannels of ~ 10 µm in diameter, perpendicularly aligned to the SZ. These channels crossed the bottom of the gel as seen in the Fig. 1B and were one millimeter long, reaching the bottom surface of the hydrogel plug.

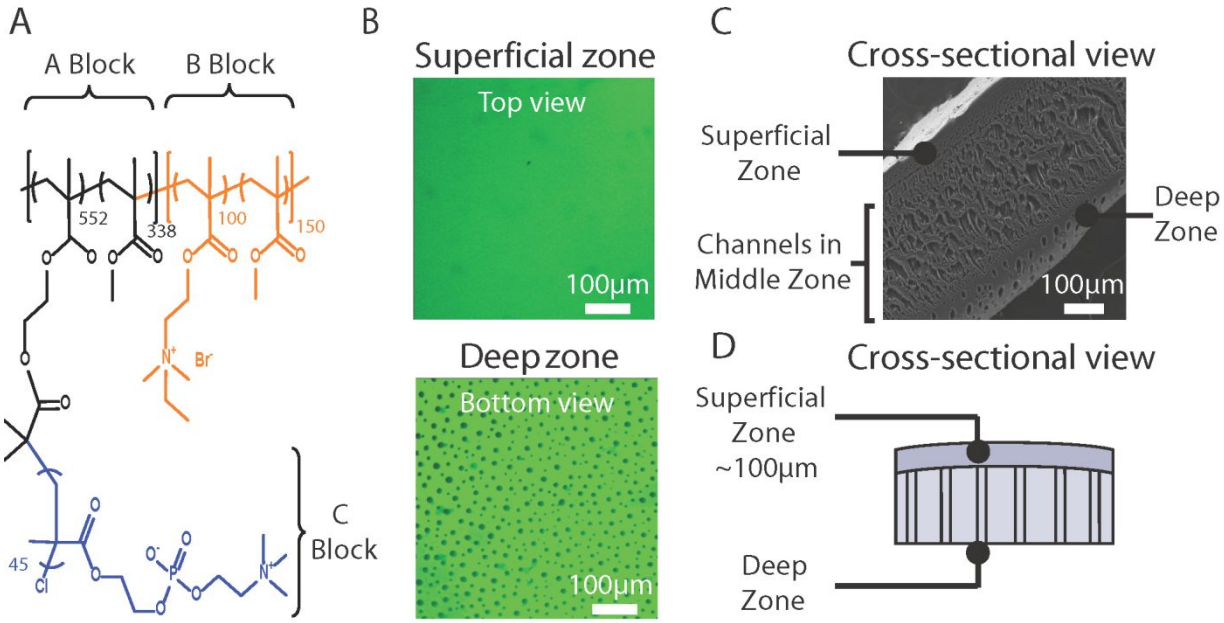

Figure 1. (A) BB polymer structure showing the three different blocks used to build the polymer, and (B) confocal microscopy imaging of the top (superficial zone) and bottom (basal zone) of the hydrogel plug (C) scanning electron microscopy micrographs of the hydrogel cross-section showing the arrangement of the different layers and structures and (D) schematic of the chitosan hydrogel plugs structure used in this study.

3.2. Tribology of gel/gel contacts in HEPES buffer

The gel friction in an aqueous buffer was assessed in two different configurations: SZ/SZ and DZ/DZ configurations (Fig. 2A). The gel disks were placed into a home-made low-load tribometer and fully immersed in a 0.1 M HEPES, 150 mM NaCl at pH 7.4. Buffered conditions were privileged since pH is known to impact the chitosan gel mechanical properties and consequently its tribological properties. In particular, a decrease of pH below or close to the pKa of amine groups of chitosan ($pK_{a\ chitosan}$ = 6.2) could trigger the chitosan chains dissolution and gel weakening. Friction forces, F_t, as a function of normal forces, F_N, were measured at a constant sliding velocity v = 5 mm/s (Fig. 2B) and as a function of sliding velocity, v, at a constant normal pressure of P = 3 kPa (Fig. 2C). To assess the speed effect, the normal pressure was set constant at 3 kPa, of the chitosan gel since it has been previously

shown that our chitosan hydrogels at a concentration of 2.5%w/w were structurally altered at normal stresses close to 30 kPa.[18]

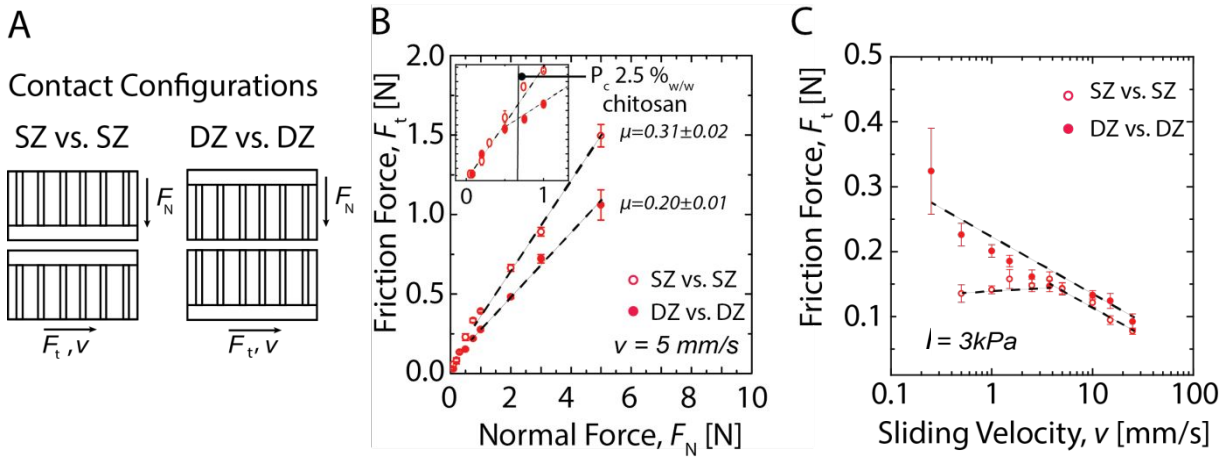

Figure 2. Tribological characterization of gel on gel flat contact in 0.1 M HEPES buffer at pH 7.4. (A) Schematic of the configurations tested (B) Friction force, F_t, as a function of applied normal force, F_N, at v = 5 mm/s for both configurations, inset is an expanded view between 0 to 1 N in order to highlight the transition between DZ and SZ configurations at the critical pressure P_c and (C) Friction force, F_t, as a function of sliding velocity, v, at P = 3kPa for both configurations.

The CoF, also denominated μ and defined as $\mu = F_t/F_N$, was higher for the SZ/SZ configuration (μ = 0.31 ± 0.02) compared to the DZ/DZ configuration (μ = 0.20 ± 0.01, Fig. 2B) in the high normal force range. No stick-slip behavior was observed in the present study as already reported for multilayered chitosan hydrogels tribopairs[18]. Such difference was observed at an applied normal pressure P_c > 6 kPa (~ 0.6 N) (see inset Fig. 2B) while at $P < P_c$, both configurations exhibited similar CoF. We previously demonstrated that the gelation process allowed the formation of a dense gel layer in the SZ characterized by a low permeability to water exudation, while the deeper zone, DZ, is composed of micron-sized channels perpendicularly aligned to the SZ[18]. The low permeability of the SZ limits the formation of a hydrodynamic water film at the rubbing contact leading to a high CoF. On contrary, at the DZ/DZ contact, the CoF was initially similar to the SZ/SZ configuration for a pressure lower

than a critical pressure ($P < P_c$). At $P > P_c$, the slope deviated to achieve a lower CoF which was due to the water exudation due to the microchannels closure into the contact from the more permeable DZ gel side.[18] This exudation was responsible for the creation of a sustainable fluid film throughout the experiment and thus improved lubrication.

Figure 2C presents the friction force as a function of the sliding velocity between two chitosan hydrogels. Both configurations exhibited different behavior when increasing the sliding velocity. Indeed, the friction force on the DZ/DZ configuration decreased monotonously with the velocity possibly indicating the presence of a mixed lubrication regime[9] since hydrogels are rough and deformable materials whereas, for the SZ/SZ configuration, the friction force was constant at $v < 5$ mm/s^{-1} and then decreased monotonically at $v > 5$ mm/s, merging toward the friction force of the DZ/DZ configuration. The behavior of the SZ/SZ configuration friction is explained by the transition from the boundary lubrication at low velocity to the mixed lubrication regime at higher velocity[48].

3.3. Lubrication with synthetic synovial fluids - Effect of the applied normal force F_N

In order to elucidate the role of the synthetic synovial fluid on the hydrogels lubrication, we firstly immersed the chitosan gels in solutions of 1 mg/mL HA of different molecular mass (10, 60, 500, and 1500 kDa) during 1 h and then tested them on the tribometer (Fig. 3 A-C). HA was used as a comparative lubricating fluid for two reasons. First, HA has a key role in the joint lubrication since it binds Agg to form a Agg/HA complexes within the cartilage, osmotically increasing the compressive modulus of cartilage as well with synovial fluid's lubricin and phospholipids to immobilize these molecules onto the shearing contact[5, 22, 49-54]. Secondly, HA is commercially used as a viscosupplement fluid for patient suffering from painful joints such as in the case osteoarthritis or directly in the eye for patients suffering from dry eye syndrom or wearing contact lenses[55-59].

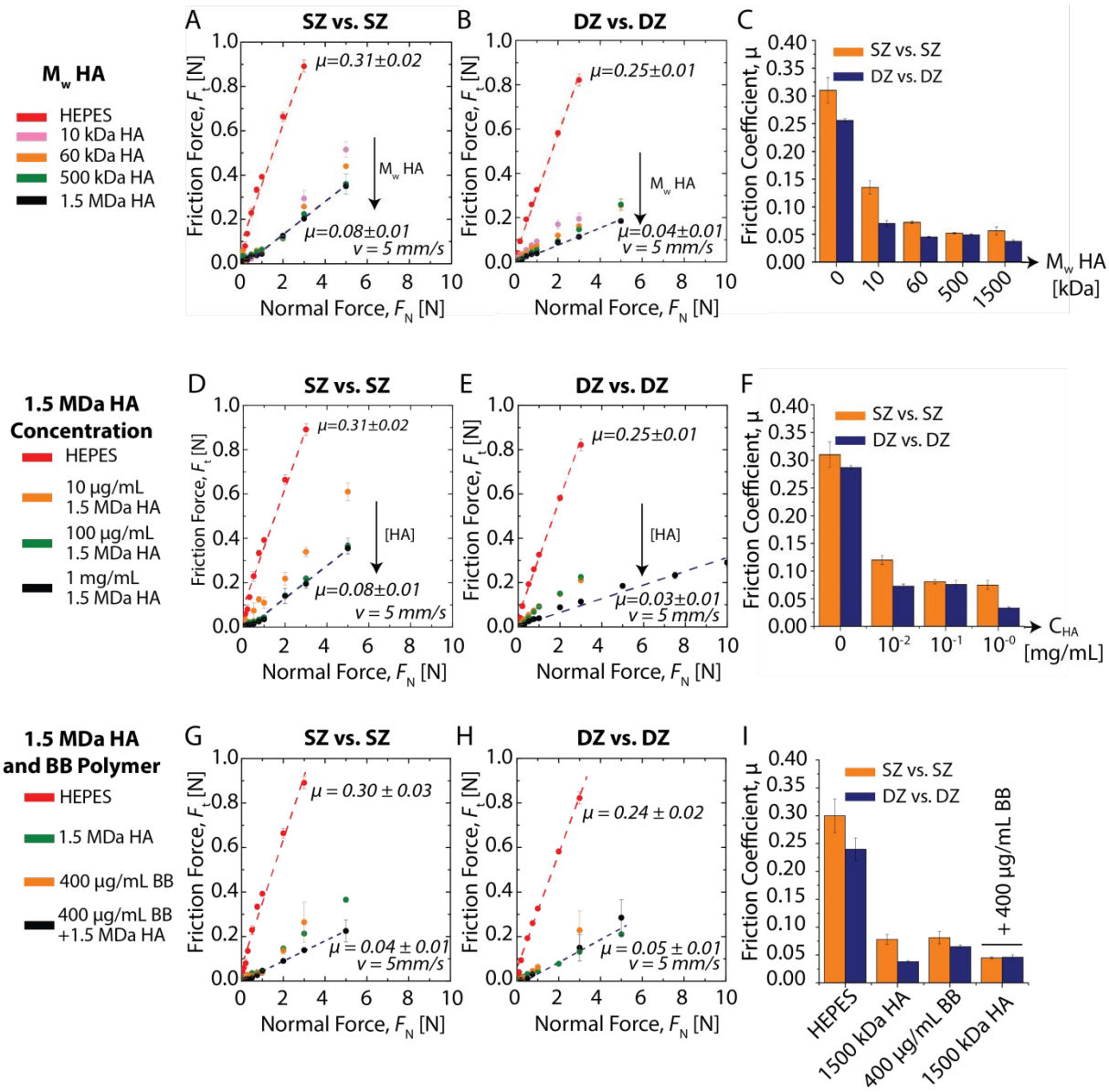

Figure 3. Measurement of the friction force, F_t, as a function of normal force, F_N, between two hydrogel plugs in presence of solutions of different molecular weights HA in the (A) SZ/SZ configuration and (B) DZ/DZ configuration. (C) Evolution of the coefficient of friction μ as a function of HA molecular weights for SZ/SZ and DZ/DZ configurations. (D) F_t as a function of F_N at different HA concentrations in the SZ/SZ configuration and the (E) DZ/DZ configuration. (F) The resulting CoF as a function of HA concentration for SZ/SZ and DZ/DZ configurations. (G) Impact of BB and HA mixtures on the friction force F_t between two hydrogel plugs in the SZ/SZ configuration and (H) DZ/DZ configuration. (I) Corresponding CoF as a function of the lubricant composition.

In both SZ/SZ and DZ/DZ configurations, the presence of HA led to a drastic decrease of the CoF compared to pure HEPES buffer (Fig. 3A and B). Once again, the DZ/DZ configuration

exhibited a slightly lower CoF, $\mu = 0.04 \pm 0.01$ for 1.5 MDa HA at $P > P_c \sim 6$ kPa in comparison with the SZ/SZ configuration exhibiting $\mu = 0.08 \pm 0.01$. The lowest HA molecular mass (10 and 60 kDa) had significantly higher CoF than the highest molecular weights in both configurations (Fig. 3C).

We then investigated the effect of high molecular weight HA concentration on the frictional behavior of chitosan gels. The gels were immersed in 1.5 MDa HA solutions of different concentrations (0, 10, 100, and 1000 μg/mL) for 1 h prior to tribo-experimentation. As seen in Fig. 3D-F, increasing HA concentration tended to decrease the CoF by one order of magnitude in both hydrogels configurations. On the SZ/SZ configuration, the CoF reached, once again a higher value ($\mu = 0.08 \pm 0.01$) than the DZ/DZ configuration, slightly merging toward gel/gel rubbing in HEPES alone for the lowest HA concentrations suggesting that low Mw HA is depleted from the contact during shearing. On the DZ/DZ configuration, the CoF remained low at $\mu = 0.04 \pm 0.01$ for $P > P_c$. These observations can be rationalized using the trapping mechanism recently reported in natural articular cartilage.[7] This mechanism considers that high molecular weight HA molecules are partially traps in cartilage collagen network under high compression which transiently immobilizes them at the interface, right where they are needed for lubrication and wear protection. A similar behavior was observed in the present system. In the DZ/DZ configuration, high molecular weight HA was effectively trapped in the pores of the interface, allowing higher lubrication compared to low molecular weight HA or to the SZ/SZ configuration. This mechanism is facilitated by the relative size of the hydrogel channels diameter (10 microns) protruding at the interface in the DZ/DZ configuration and the radius of gyration of HA molecules ($R_g = 154 \pm 12$ nm at 1.5 MDa buffered saline).

The BB polymer alone presented a similar behavior to high molecular HA, which is not surprising since BB is also a high molecular weight polymer (Mw ≈ 10^7 g/mol, Fig. 3G and H). At a concentration of 400 µg/mL, the CoF of the BB polymer solution was $\mu = 0.08 \pm 0.01$ in the SZ/SZ configuration compared to 0.05 ± 0.01 in the DZ/DZ configuration.(Fig 3G-I). Finally, the BB polymer at 400 µg/mL was mixed to the 1.5 MDa HA solution and tribogically tested on both hydrogel configurations. To increase interaction with 1.5 MDa HA, a small polycationic attachment group (Fig. 1A, B block) was grafted on a linear domain to mimic proteoglycan attachment groups onto HA. Figure 3G shows that the CoF in SZ/SZ configuration (which was systematically the highest, independently of the HA used) was lowered using the macromolecules mixture ($\mu = 0.04 \pm 0.01$), reaching values similar to those observed for the DZ/DZ configuration (Fig 3H) with the 1.5 MDa HA at 1 mg/mL. In contrast, the effect of the mixture was unnoticeable in the DZ/DZ configuration since no significant differences in CoF were observed compared to 1.5 MDa HA at 1 mg/mL alone. Therefore, the BB polymer combined with high molecular weight HA allows to obtain a CoF that is independent of the hydrogel configuration, smearing out the effect of the interface structure.

The last observation indicates that the synergistic interaction between HA and the BB polymer allows the lubricant to remain in the shear contact even in the absence of any surface pores. We previously showed that BB polymers without any polycationic side block could entangle with HA macromolecules under confinement creating a strongly cohesive lubricating interfacial film.[33] The presence of a polycationic side block in the BB polymer we used in this study drastically enhances the interaction between both polymers even under low applied load which helps maintaining them in the interfacial contact even under high shear conditions.

3.4. Lubrication with synthetic synovial fluids - Effect of the sliding velocity, v

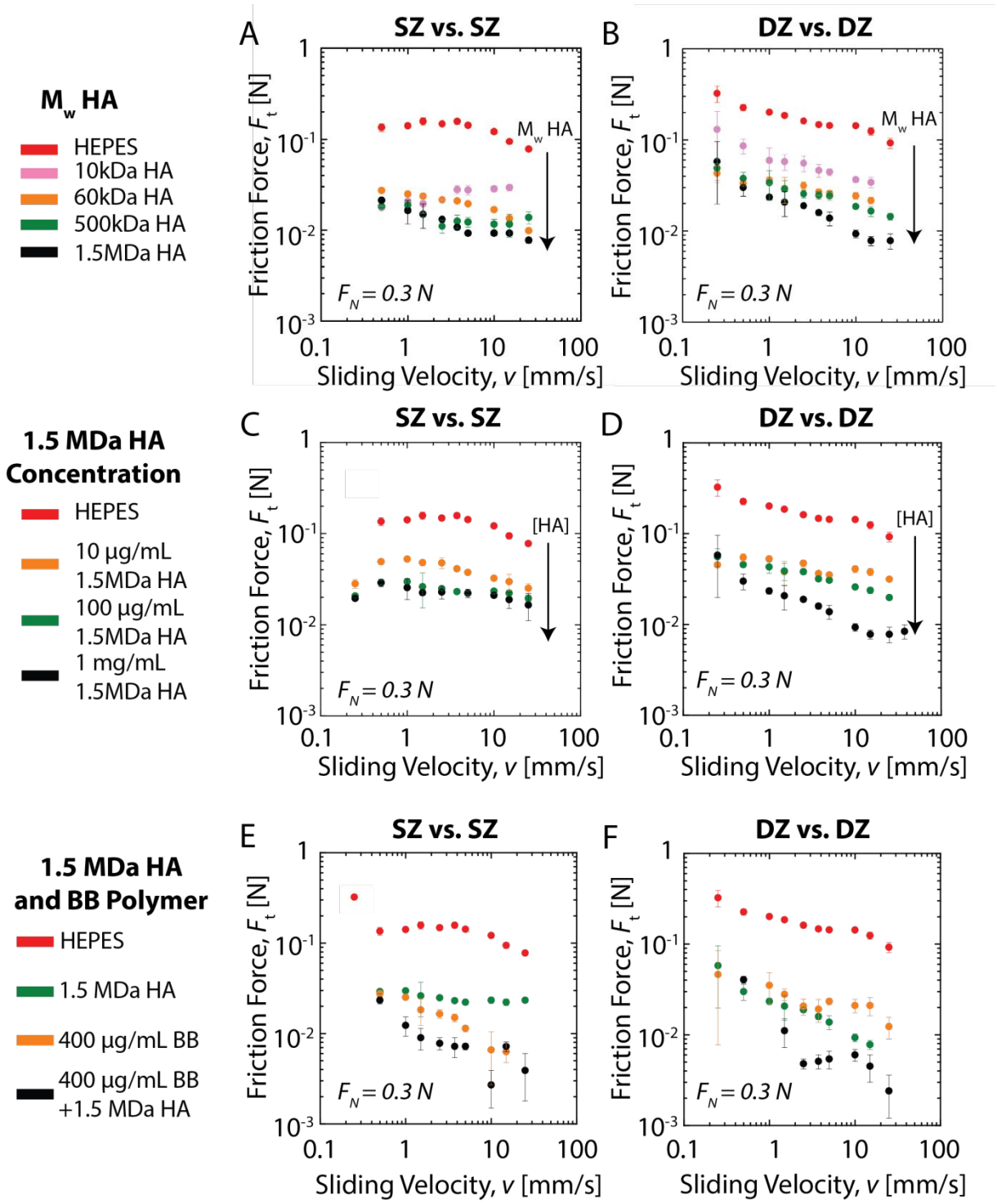

Figure 4. Measurement of the friction force, F_t, as a function of the sliding velocity, v, to assess the effect of HA molecular mass (10, 60, 500 and 1500 kDa) at a fixed concentration of 1 mg/mL for the (A) SZ/SZ configuration and (B) DZ/DZ configuration. Measurement of F_t vs. v to assess the effect of HA concentration for the (C) SZ/SZ configuration and (D) DZ/DZ configuration. Measurement of F_t vs. v to assess the effect of 1.5 MDa HA at 1 mg/mL in combination with BB polymer for the (E) SZ/SZ configuration and (F) DZ/DZ configuration. Gels were immersed for 1 h in the synthetic synovial fluids prior to start the tribotests.

The effect of the sliding velocity on the friction forces for the chitosan hydrogels plugs in the SZ/SZ and DZ/DZ configurations using different lubricating fluids is presented in Fig. 4. In these experiments, the applied normal load was set constant at P = 3 kPa < P_c. In both configurations and for each lubricating system, the friction force was decreased by one order of magnitude when HA, BB or HA and BB mixture were used compared to HEPES buffer only, suggesting a substantial role of these polymers on the lubrication at the gel/gel interface. Concerning the effect of HA molecular weight (Fig. 4A-B), both configurations showed different behaviors upon increasing the sliding velocity. The SZ/SZ configuration exhibited a friction force almost independent of the velocity for low sliding velocities[60-61], indicating the mechanism of boundary lubrication regime, since the friction forces did not depend on the physical properties of the gel nor on the lubricant viscosity, but only on the chemical composition of the surface/adsorbed molecules (Fig. 4A). The DZ/DZ configuration exhibited a monotonous decrease of the friction force suggesting a mixed lubrication mechanism due to the mixed load support by the lubricating film and local asperities on the hydrogels contact[48]. At low velocity, the friction force was slightly lower on the SZ/SZ configuration than the DZ/DZ configuration for low molecular weight HA. This might be due to the larger roughness of the DZ surface (see latter in the wear study section) which could lead to a higher friction[48]. This difference readily vanished upon increasing the sliding velocity and the friction force became even lower on the DZ/DZ configuration at v > 10 mm/s (Fig. 4B). Increase of HA concentration tended to dramatically decrease the friction force (Fig. 4 C-D) independently of the hydrogel configuration used. The evolution of the friction force with the sliding speed measured at different HA concentrations of 1.5 MDa HA shows that boundary lubrication is the dominating regime in the SZ/SZ configuration while a mixed lubrication is possibly occurring in the DZ/DZ configuration.

The effect of the sliding velocity in presence of BB polymer alone is presented in Fig. 4 E-F. On both configurations, the frictions forces decreased monotonously with the increase of the sliding velocity and where lower in the SZ/SZ configuration than in the DZ/DZ configuration. This behavior has been reported for similar systems composed of grafted pMPC brushes[62]. This monotonous behavior was conserved when BB polymer was mixed with high molecular weight HA. However, the friction forces of the mixture were systematically lower than HA or BB alone at sliding speed greater than 1 mm/s which indicates a synergy between both polymers (Fig. 4 E-F). At low sliding speed, it appears that the friction forces of HA, BB polymer and their mixture converge toward a high value friction force that depends on the testing configurations.

3.5. Hydrogel wear protection with synthetic synovial fluids - visualization and characterization

The structural integrity of the chitosan hydrogels surfaces was systematically monitored to highlight the role of the bioinspired synovial fluid on wear protection. The evaluation of wear debris volume was not possible in set up configuration we used, therefore wear damage was first qualitatively analyzed by the means of a digital microscope and quantitatively analyzed after tribotesting using interferometric microscopy. For wear experiments, hydrogels were mounted in the same SZ/SZ and DZ/DZ configurations as in the lubrication study. Imaging of the hydrogel plugs was performed after 10000 cycles of back and forth motion at an applied pressure P = 30 kPa in an aqueous solution fixed at pH 7.4 with a constant sliding speed of 5 mm/s at a frequency of 1 Hz. It was previously shown that multilayered chitosan hydrogels under shearing suffered from destruction at a pressure close to their shear modulus at the DZ/DZ configurations. Images of the 21 mm hydrogel plugs are shown in Fig. 5. The 11 mm hydrogel plugs displayed similar surface features after wear tests and were not presented for

clarity. These images show that without any lubricant macromolecules, the chitosan gels displayed severe surface damage when tested in the DZ/DZ configuration and showed surface polishing / abrasion in the SZ/SZ configuration. Interferometric images on damaged surfaces presented large dark areas indicating the presence of deep crevices far too high to be measurable by this technique. Lubricating fluids containing HA at 1 mg/mL, exhibited M_w -dependent wear protection in the DZ/DZ configuration. High molecular mass HA solution (M_w = 1.5 MDa) protected the hydrogel plugs significantly more than low molecular mass HA (M_w = 10 kDa) in the DZ/DZ configuration while differences in wear protection in the SZ/SZ configuration were much less significant. These observations highlight the important role of the hydrogel interfacial structure in controlling wear initiation and propagation in presence of linear polymer lubricants. As seen in Fig. 5, the BB polymer alone was able to protect the hydrogel plugs very similarly to high molecular weight HA solutions with only few defects appearing on both tested configurations. The mixture of BB polymer along with high molecular mass HA (M_w = 1.5 MDa) showed very little wear on both SZ and DZ surfaces compared to the initial surfaces.

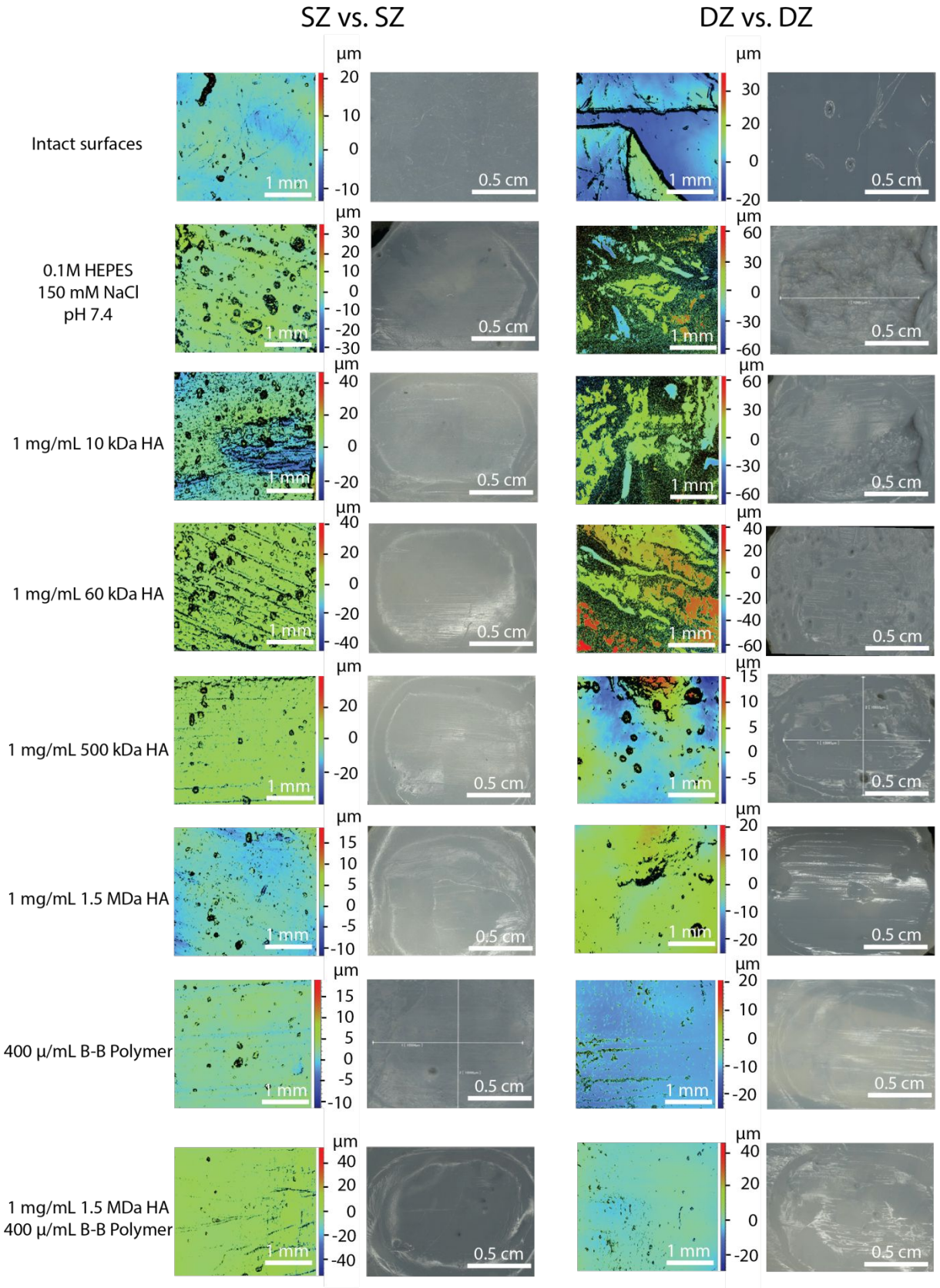

Figure 5. Interferometric and digital imaging of chitosan hydrogel plugs after 10^4 cycles at P = 30 kPa, v = 5 mm/s and a frequency of 1 Hz using different fluid compositions and hydrogels configurations. Certain panels are reproduced from Ref. 18 with permission from the Royal Society of Chemistry.

Using optical interferometry, the roughness in the wear tracks was evaluated after tribotesting (Fig. 6). The arithmetical mean height of the whole gel surfaces, S_a, was used as the parameter characterizing the roughness before and after wear tests. This parameter corresponds to the absolute difference of the height of each point of a surface to the arithmetical mean of the gel surface. Before wear tests, the initial roughness of the chitosan hydrogel plugs (Intact surfaces in Fig. 6) was higher on the DZ side (S_a = 4 µm) than on the SZ side (S_a = 0.8 µm). When using only HEPES as a lubricating fluid, the final roughness of the chitosan hydrogels was significantly higher on both configurations since S_a increased to 2.5 µm on the SZ side and was impossible to measure on the DZ side due to strong damage of the gel (S_a >> 16 µm). When using HA-based fluids, the final gel roughness was significantly smaller than HEPES and decreased with HA molecular weight. Upon the addition of the BB polymer to the high molecular weight HA solution, the final roughness was finally equal to the initial value for the SZ/SZ configuration and lower than the initial value for the DZ/DZ configuration, possibly due to surface heterogeneities leveling upon gel rubbing.

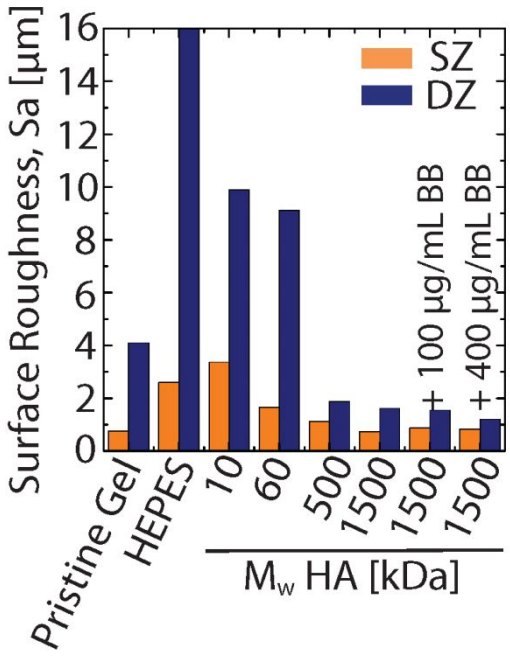

Figure 6. Quantitative wear assessment by the means of surface roughness, S_a, of gel sample after wear experiment as a function of immersion bath composition for both contact

configuration measured by interferometry

4. Conclusions

The present study shows that a lubricating fluid composed of BB polymer and high molecular weight HA is able to efficiently provide concomitantly wear protection of soft and porous materials and decrease the CoF, for different surface topographies or structures. These results anticipate the potential use of such lubricating fluid for various biomedical applications such as joints viscosupplementation or eyes and contact lenses hydration and lubrication.

Author Information

corresponding authors

*laurent.david@univ-lyon.fr

*xavier.banquy@umontreal.ca

Notes

The authors declare no competing financial interest.

Acknowledgements

JF is grateful to the Arthritis Society, the Faculté des études supérieures et postdoctorales from the Université de Montréal and the French Embassy (Frontenac scholarship) for financial supports. BRS thanks the financial support of GRUM. XB acknowledges the financial support from the Canada research chair program and NSERC (Discovery grant). XB and GS are grateful for the financial support of the FRQNT-CFQCU (Samuel de Champlain grant). KM Acknowledges support from NSF (DMR 1501324). We thank Agnes Crépet (IMP) and Pierre Alcouffe (IMP) for their technical assistance in size exclusion chromatography and scanning electron microscopy, respectively. The help of Matthieu Guibert (LTDS) for the low-load tribometer design and fabrication, Thomas Malhomme (LTDS) for wear analysis by interferometry, and Béatrice Burdin (Centre Technologique des Microstructures) for CLSM study implementation is also acknowledged.

References

(1) Spiller, K. L.; Maher, S. A.; Lowman, A. M. Hydrogels for the Repair of Articular Cartilage Defects. *Tissue Eng., Part B* **2011,** *17*, 281-299.
(2) Montembault, A.; Tahiri, K.; Korwin-Zmijowska, C.; Chevalier, X.; Corvol, M. T.; Domard, A. A material decoy of biological media based on chitosan physical hydrogels: application to cartilage tissue engineering. *Biochimie* **2006,** *88*, 551-564.
(3) Makris, E. A.; Gomoll, A. H.; Malizos, K. N.; Hu, J. C.; Athanasiou, K. A. Repair and tissue engineering techniques for articular cartilage. *Nat. Rev. Rheumatol.* **2015,** *11*, 21-34.
(4) Greene, G. W.; Banquy, X.; Lee, D. W.; Lowrey, D. D.; Yu, J.; Israelachvili, J. N. Adaptive mechanically controlled lubrication mechanism found in articular joints. *Proc. Natl. Acad. Sci. U. S. A.* **2011,** *108*, 5255-5259.
(5) Das, S.; Banquy, X.; Zappone, B.; Greene, G. W.; Jay, G. D.; Israelachvili, J. N. Synergistic interactions between grafted hyaluronic acid and lubricin provide enhanced wear protection and lubrication. *Biomacromolecules* **2013,** *14*, 1669-1677.
(6) Greene, G. W.; Zappone, B.; Zhao, B.; Soderman, O.; Topgaard, D.; Rata, G.; Israelachvili, J. N. Changes in pore morphology and fluid transport in compressed articular cartilage and the implications for joint lubrication. *Biomaterials* **2008,** *29*, 4455-4462.
(7) Greene, G. W.; Zappone, B.; Soderman, O.; Topgaard, D.; Rata, G.; Zeng, H.; Israelachvili, J. N. Anisotropic dynamic changes in the pore network structure, fluid diffusion and fluid flow in articular cartilage under compression. *Biomaterials* **2010,** *31*, 3117-3128.
(8) Forster, H.; Fisher, J. The Influence of Loading Time and Lubricant on the Friction of Articular Cartilage. *Proc. Inst. Mech. Eng., Part H* **1996,** *210*, 109-119.
(9) Jahn, S.; Seror, J.; Klein, J. Lubrication of Articular Cartilage. *Annu. Rev. Biomed. Eng.* **2016,** *18*, 235-258.
(10) Ateshian, G. A. The role of interstitial fluid pressurization in articular cartilage lubrication. *J. Biomech.* **2009,** *42*, 1163-1176.
(11) Klein, J. Molecular mechanisms of synovial joint lubrication. *Proc. Inst. Mech. Eng., Part J* **2006,** *220*, 691-710.
(12) Balazs, E. A. The role of hyaluronan in the structure and function of the biomatrix of connective tissues. *Struct. Chem.* **2009,** *20*, 233-243.
(13) Lin, P.; Zhang, R.; Wang, X.; Cai, M.; Yang, J.; Yu, B.; Zhou, F. Articular Cartilage Inspired Bilayer Tough Hydrogel Prepared by Interfacial Modulated Polymerization Showing Excellent Combination of High Load-Bearing and Low Friction Performance. *ACS Macro Lett.* **2016,** *5*, 1191-1195.
(14) Yashima, S.; Takase, N.; Kurokawa, T.; Gong, J. P. Friction of hydrogels with controlled surface roughness on solid flat substrates. *Soft Matter* **2014,** *10*, 3192-9.
(15) Khosla, T.; Cremaldi, J.; Erickson, J. S.; Pesika, N. S. Load-Induced Hydrodynamic Lubrication of Porous Films. *ACS Appl. Mater. Interfaces* **2015,** *7*, 17587-17591.
(16) Gong, J. P. Friction and lubrication of hydrogels-its richness and complexity. *Soft Matter* **2006,** *2*, 544-552.
(17) Singh, A.; Corvelli, M.; Unterman, S. A.; Wepasnick, K. A.; McDonnell, P.; Elisseeff, J. H. Enhanced lubrication on tissue and biomaterial surfaces through peptide-mediated binding of hyaluronic acid. *Nat. Mater.* **2014,** *13*, 988-995.
(18) Faivre, J.; Sudre, G.; Montembault, A.; Benayoun, S.; Banquy, X.; Delair, T.; David, L. Bioinspired Microstructures of Chitosan Hydrogel Provide Enhanced Wear Protection. *Soft Matter* **2018**, 2068-2076.
(19) Zhang, R.; Feng, Y.; Ma, S.; Cai, M.; Yang, J.; Yu, B.; Zhou, F. Tuning the Hydration and Lubrication of the Embedded Load-Bearing Hydrogel Fibers. *Langmuir* **2017,** *33*, 2069-2075.
(20) Ohsedo, Y.; Takashina, R.; Gong, J. P.; Osada, Y. Surface Friction of Hydrogels with Well-Defined Polyelectrolyte Brushes. *Langmuir* **2004,** *20*, 6549-6555.

(21) Kamada, K.; Furukawa, H.; Kurokawa, T.; Tada, T.; Tominaga, T.; Nakano, Y.; Gong, J. P. Surfactant-induced friction reduction for hydrogels in the boundary lubrication regime. *J. Phys.: Condens. Matter* **2011,** *23*, 284107.
(22) Samsom, M.; Iwabuchi, Y.; Sheardown, H.; Schmidt, T. A. Proteoglycan 4 and hyaluronan as boundary lubricants for model contact lens hydrogels. *J. Biomed. Mater. Res. B Appl. Biomater.* **2017**, 1329-1338.
(23) McGann, M. E.; Bonitsky, C. M.; Jackson, M. L.; Ovaert, T. C.; Trippel, S. B.; Wagner, D. R. Genipin crosslinking of cartilage enhances resistance to biochemical degradation and mechanical wear. *J. Orthop. Res.* **2015,** *33*, 1571-1579.
(24) Liao, I. C.; Moutos, F. T.; Estes, B. T.; Zhao, X.; Guilak, F. Composite Three-Dimensional Woven Scaffolds with Interpenetrating Network Hydrogels to Create Functional Synthetic Articular Cartilage. *Adv. Funct. Mater.* **2013,** *23*, 5833-5839.
(25) Yasuda, K.; Ping Gong, J.; Katsuyama, Y.; Nakayama, A.; Tanabe, Y.; Kondo, E.; Ueno, M.; Osada, Y. Biomechanical properties of high-toughness double network hydrogels. *Biomaterials* **2005,** *26*, 4468-4475.
(26) Nakajima, T. Generalization of the sacrificial bond principle for gel and elastomer toughening. *Polym. J.* **2017,** *49*, 477-485.
(27) Kolmakov, G. V.; Matyjaszewski, K.; Balazs, A. C. Harnessing labile bonds between nanogel particles to create self-healing materials. *ACS Nano* **2009,** *3*, 885-892.
(28) Faivre, J.; Shrestha, B. R.; Xie, G.; Olszewski, M.; Adibnia, V.; Moldovan, F.; Montembault, A.; Sudre, G.; Delair, T.; David, L.; Matyjaszewski, K.; Banquy, X. Intermolecular Interactions between Bottlebrush Polymers Boost the Protection of Surfaces against Frictional Wear. *Chem. Mater.* **2018,** *30*, 4410-9.
(29) Lee, H.-i.; Pietrasik, J.; Sheiko, S. S.; Matyjaszewski, K. Stimuli-responsive molecular brushes. *Prog. Polym. Sci.* **2010,** *35*, 24-44.
(30) Matyjaszewski, K. Atom Transfer Radical Polymerization (ATRP): Current Status and Future Perspectives. *Macromolecules* **2012,** *45*, 4015-4039.
(31) Schmidt, T. A.; Gastelum, N. S.; Nguyen, Q. T.; Schumacher, B. L.; Sah, R. L. Boundary lubrication of articular cartilage: Role of synovial fluid constituents. *Arthritis & Rheumatism* **2007,** *56*, 882-891.
(32) Banquy, X.; Burdyńska, J.; Lee, D. W.; Matyjaszewski, K.; Israelachvili, J. Bioinspired Bottle-Brush Polymer Exhibits Low Friction and Amontons-like Behavior. *J. Am. Chem. Soc.* **2014,** *136*, 6199-6202.
(33) Faivre, J.; Shrestha, B. R.; Burdynska, J.; Xie, G.; Moldovan, F.; Delair, T.; Benayoun, S.; David, L.; Matyjaszewski, K.; Banquy, X. Wear Protection without Surface Modification Using a Synergistic Mixture of Molecular Brushes and Linear Polymers. *ACS Nano* **2017,** *11*, 1762-1769.
(34) Faivre, J.; Shrestha, B. R.; Xie, G.; Delair, T.; David, L.; Matyjaszewski, K.; Banquy, X. Unraveling the Correlations between Conformation, Lubrication, and Chemical Stability of Bottlebrush Polymers at Interfaces. *Biomacromolecules* **2017**, 4002-4010.
(35) Pan, Y.-S.; Xiong, D.-S.; Ma, R.-Y. A study on the friction properties of poly(vinyl alcohol) hydrogel as articular cartilage against titanium alloy. *Wear* **2007,** *262*, 1021-1025.
(36) Choi, S. H.; Park, K. S.; Sung, M. W.; Kim, K. H. Dynamic and quantitative evaluation of eyelid motion using image analysis. *Med Biol Eng Comput* **2003,** *41*, 146-50.
(37) Bentivoglio, A. R.; Bressman, S. B.; Cassetta, E.; Carretta, D.; Tonali, P.; Albanese, A. Analysis of blink rate patterns in normal subjects. *Mov. Disord.* **1997,** *12*, 1028-34.
(38) Delmotte, P.; Sanderson, M. J. Ciliary Beat Frequency Is Maintained at a Maximal Rate in the Small Airways of Mouse Lung Slices. *Am. J. Respir. Cell Mol. Biol.* **2006,** *35*, 110-117.
(39) Oldenburg, A. L.; Chhetri, R. K.; Hill, D. B.; Button, B. Monitoring airway mucus flow and ciliary activity with optical coherence tomography. *Biomedical Optics Express* **2012,** *3*, 1978-1992.
(40) Dedinaite, A. Biomimetic lubrication. *Soft Matter* **2012,** *8*, 273-284.

(41) Elsaid, K. A.; Fleming, B. C.; Oksendahl, H. L.; Machan, J. T.; Fadale, P. D.; Hulstyn, M. J.; Shalvoy, R.; Jay, G. D. Decreased lubricin concentrations and markers of joint inflammation in the synovial fluid of patients with anterior cruciate ligament injury. *Arthritis Rheum.* **2008,** *58*, 1707-1715.
(42) Hilbert, B. J.; Rowley, G.; Antonas, K. N. Hyaluronic acid concentration in synovial fluid from normal and arthritic joints of horses. *Aust. Vet. J.* **1984,** *61*, 22-24.
(43) Tamer, T. M. Hyaluronan and synovial joint: function, distribution and healing. *Interdiscip. Toxicol.* **2013,** *6*, 111-125.
(44) Lee, D. W.; Banquy, X.; Das, S.; Cadirov, N.; Jay, G.; Israelachvili, J. Effects of molecular weight of grafted hyaluronic acid on wear initiation. *Acta Biomater.* **2014,** *10*, 1817-1823.
(45) Nie, J.; Lu, W.; Ma, J.; Yang, L.; Wang, Z.; Qin, A.; Hu, Q. Orientation in multi-layer chitosan hydrogel: morphology, mechanism, and design principle. *Sci. Rep.* **2015,** *5*, 7635.
(46) Fiamingo, A.; Montembault, A.; Boitard, S.-E.; Naemetalla, H.; Agbulut, O.; Delair, T.; Campana-Filho, S. P.; Menasché, P.; David, L. Chitosan Hydrogels for the Regeneration of Infarcted Myocardium: Preparation, Physicochemical Characterization, and Biological Evaluation. *Biomacromolecules* **2016,** *17*, 1662-1672.
(47) Sereni, N.; Enache, A.; Sudre, G.; Montembault, A.; Rochas, C.; Durand, P.; Perrard, M. H.; Bozga, G.; Puaux, J. P.; Delair, T.; David, L. Dynamic Structuration of Physical Chitosan Hydrogels. *Langmuir* **2017,** *33*, 12697-12707.
(48) Yashima, S.; Takase, N.; Kurokawa, T.; Gong, J. P. Friction of hydrogels with controlled surface roughness on solid flat substrates. *Soft Matter* **2014,** *10*, 3192-3199.
(49) Kawano, T.; Miura, H.; Mawatari, T.; Moro-Oka, T.; Nakanishi, Y.; Higaki, H.; Iwamoto, Y. Mechanical effects of the intraarticular administration of high molecular weight hyaluronic acid plus phospholipid on synovial joint lubrication and prevention of articular cartilage degeneration in experimental osteoarthritis. *Arthritis and rheumatism* **2003,** *48*, 1923-9.
(50) Liu, C.; Wang, M.; An, J.; Thormann, E.; Dedinaite, A. Hyaluronan and phospholipids in boundary lubrication. *Soft Matter* **2012,** *8*, 10241-10244.
(51) Chang, D. P.; Abu-Lail, N. I.; Guilak, F.; Jay, G. D.; Zauscher, S. Conformational Mechanics, Adsorption, and Normal Force Interactions of Lubricin and Hyaluronic Acid on Model Surfaces. *Langmuir* **2008,** *24*, 1183-1193.
(52) Teeple, E.; Elsaid, K. A.; Jay, G. D.; Zhang, L.; Badger, G. J.; Akelman, M.; Bliss, T. F.; Fleming, B. C. Effects of supplemental intra-articular lubricin and hyaluronic acid on the progression of posttraumatic arthritis in the anterior cruciate ligament-deficient rat knee. *Am. J. Sports Med.* **2011,** *39*, 164-72.
(53) Majd, S. E.; Kuijer, R.; Kowitsch, A.; Groth, T.; Schmidt, T. A.; Sharma, P. K. Both Hyaluronan and Collagen Type II Keep Proteoglycan 4 (Lubricin) at the Cartilage Surface in a Condition That Provides Low Friction during Boundary Lubrication. *Langmuir* **2014**, 14566-14572.
(54) Bonnevie, E. D.; Galesso, D.; Secchieri, C.; Cohen, I.; Bonassar, L. J. Elastoviscous Transitions of Articular Cartilage Reveal a Mechanism of Synergy between Lubricin and Hyaluronic Acid. *PLOS ONE* **2015,** *10*, e0143415.
(55) Masuko, K.; Murata, M.; Yudoh, K.; Kato, T.; Nakamura, H. Anti-inflammatory effects of hyaluronan in arthritis therapy: Not just for viscosity. *Int. J. Gen. Med.* **2009,** *2*, 77-81.
(56) Bailleul, F., Regimens for intra-articular viscosupplementation. Google Patents: 2011.
(57) Ammar, T. Y.; Pereira, T. A. P.; Mistura, S. L. L.; Kuhn, A.; Saggin, J. I.; Lopes Júnior, O. V. Viscosupplementation for treating knee osteoarthrosis: review of the literature. *Revista Brasileira de Ortopedia* **2015,** *50*, 489-494.
(58) Samsom, M. L.; Morrison, S.; Masala, N.; Sullivan, B. D.; Sullivan, D. A.; Sheardown, H.; Schmidt, T. A. Characterization of full-length recombinant human Proteoglycan 4 as an ocular surface boundary lubricant. *Exp. Eye Res.* **2014,** *127*, 14-9.
(59) Lambiase, A.; Sullivan, B. D.; Schmidt, T. A.; Sullivan, D. A.; Jay, G. D.; Truitt, E. R., 3rd; Bruscolini, A.; Sacchetti, M.; Mantelli, F. A Two-Week, Randomized, Double-masked Study to Evaluate Safety

and Efficacy of Lubricin (150 mug/mL) Eye Drops Versus Sodium Hyaluronate (HA) 0.18% Eye Drops (Vismed(R)) in Patients with Moderate Dry Eye Disease. *Ocul Surf* **2017,** *15*, 77-87.
(60) Oogaki, S.; Kagata, G.; Kurokawa, T.; Kuroda, S.; Osada, Y.; Gong, J. P. Friction between like-charged hydrogels-combined mechanisms of boundary, hydrated and elastohydrodynamic lubrication. *Soft Matter* **2009,** *5*, 1879-1887.
(61) Chang, D. P.; Abu-Lail, N. I.; Coles, J. M.; Guilak, F.; Jay, G. D.; Zauscher, S. Friction force microscopy of lubricin and hyaluronic acid between hydrophobic and hydrophilic surfaces. *Soft Matter* **2009,** *5*, 3438-3445.
(62) Kobayashi, M.; Takahara, A. Tribological properties of hydrophilic polymer brushes under wet conditions. *Chem. Rec.* **2010,** *10*, 208-216.

Table of Contents

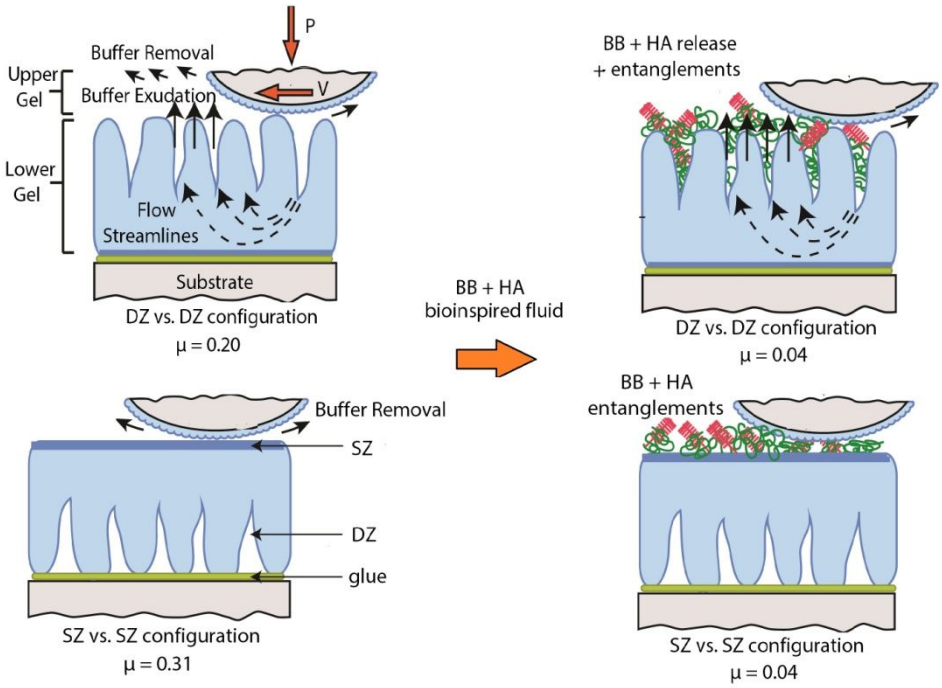

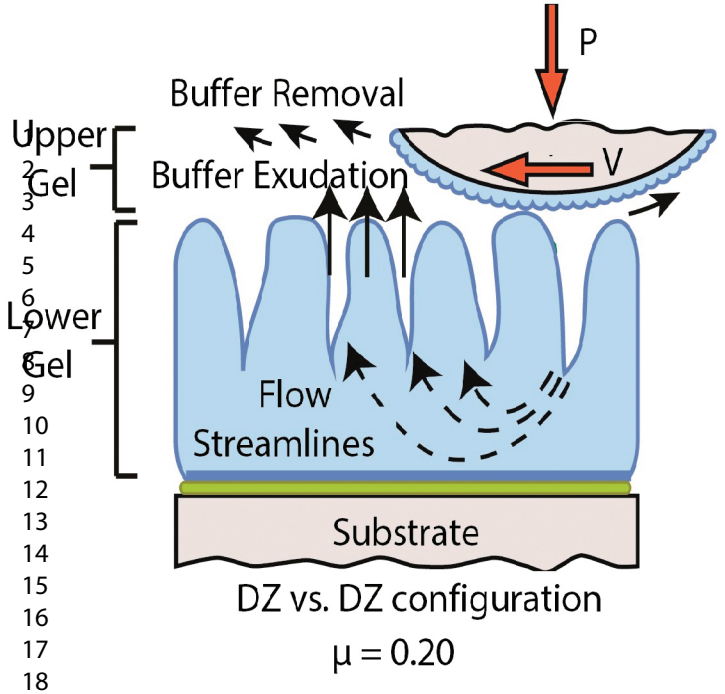

DZ vs. DZ configuration

$\mu = 0.20$

BB + HA bioinspired fluid

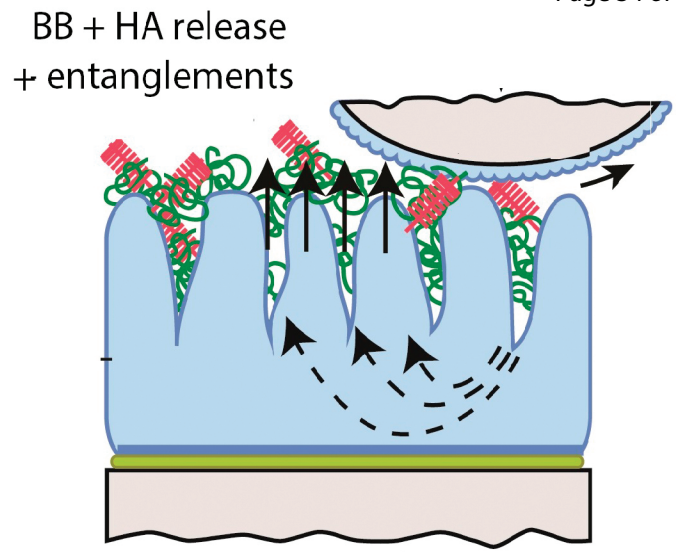

DZ vs. DZ configuration

$\mu = 0.04$

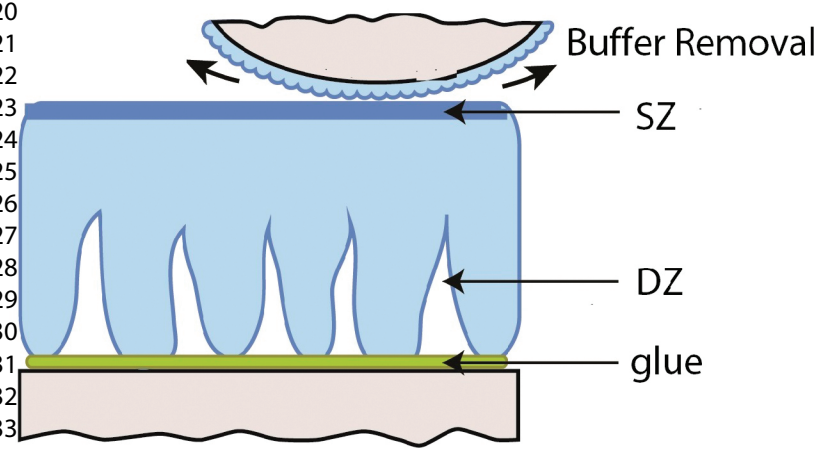

SZ vs. SZ configuration

$\mu = 0.31$

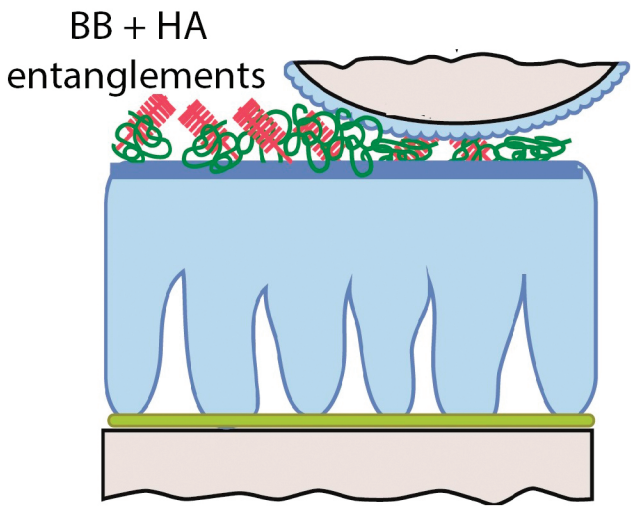

SZ vs. SZ configuration

$\mu = 0.04$